ACS SyntheticBiology

Research Article

pubs.acs.org/synthbio

# Memory and Combinatorial Logic Based on DNA Inversions: Dynamics and Evolutionary Stability

Jesus Fernandez-Rodriguez,[†] Lei Yang,[†] Thomas E. Gorochowski,[†] D. Benjamin Gordon,[†,‡] and Christopher A. Voigt*[,†,‡]

[†]Synthetic Biology Center, Department of Biological Engineering, Massachusetts Institute of Technology, Cambridge, Massachusetts 02139, United States

[‡]Broad Institute of MIT and Harvard, Cambridge, Massachusetts 02142, United States

Supporting Information

**ABSTRACT:** Genetic memory can be implemented using enzymes that catalyze DNA inversions, where each orientation corresponds to a "bit". Here, we use two DNA invertases (FimE and HbiF) that reorient DNA irreversibly between two states with opposite directionality. First, we construct memory that is set by FimE and reset by HbiF. Next, we build a NOT gate where the input promoter drives FimE and in the absence of signal the reverse state is maintained by the constitutive expression of HbiF. The gate requires ∼3 h to turn on and off. The evolutionary stabilities of these circuits are measured by passaging cells while cycling function. The memory switch is stable over 400 h (17 days, 14 state changes); however, the gate breaks after 54 h (>2 days) due to continuous invertase expression. Genome sequencing reveals that the circuit remains intact, but the host strain evolves to reduce invertase expression. This work highlights the need to evaluate the evolutionary robustness and failure modes of circuit designs, especially as more complex multigate circuits are implemented.

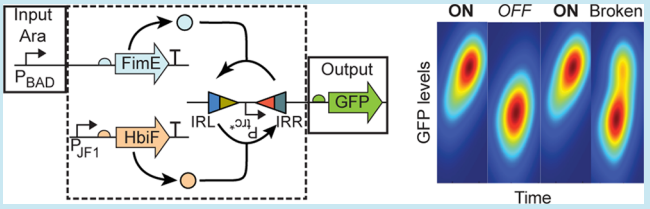


**KEYWORDS:** *synthetic biology, systems biology, genetic circuit, genetic compiler, design automation*



Recombinases are enzymes that physically rearrange DNA. In their natural context, they have roles in mobile element transit, creating phenotypic diversity and regulating gene expression.[1−6] The DNA changes catalyzed by recombinases can be viewed as states; for example, some can invert a region of DNA between two orientations each of which corresponds to a state.[4,5,7−12] As such, they have been co-opted by engineers to build synthetic genetic circuits. Their advantage is that they can hold a state that can be read later, even after the cell dies, without the continuous expression of a regulator. For example, it can be connected to an inducible system so that the output remains on even after the removal of inducer.[13,14] This can serve as a form of memory so that a transient input stimulus is permanently recorded. Circuits have been built based on multiple recombinases that can perform counting and sequential logic.[15−18] Various applications of memory have been proposed, including a permanent switch when bacteria sense stimuli in the gut,[19,20] to record the presence of markers as a urine diagnostic,[21,22] and to switch between metabolic states in yeast.[23]

These circuits have been built based on several classes of recombinases. The first are reversible recombinases (*e.g.*, cre) that catalyze both the forward and reverse changes in orientation, as the recognition site is unaltered after inversion.[1] When the recombinase is continuously expressed, this can lead to a mixed distribution across a population at steady-state.[1,24,25] The second are irreversible recombinases that only catalyze one orientation change because the recognition site changes after the switch.[5,13,14,26−28] This approach is scalable; for example, we showed that a "memory array" could be built that can record up to 12 events using orthogonal recombinases.[29] The challenge with irreversible recombinases is that the switch is permanent and there is no way to reset back to the original state without rebuilding the DNA. To address this, Endy and co-workers built a "set:reset" switch based on an integrase:excisionase pair.[30] When only the integrase is expressed, this biases the switch in one direction, but when it is coexpressed with the excisionase, this biases it in the other direction. The only challenge in working with this system is that one protein participates in both orientation changes, thus requiring careful tuning of expression.

Circuits that implement logic operations have been built using irreversible recombinases.[18,31] Promoters that serve as inputs drive the expression of a pair of irreversible recombinases and the logic is implemented by the pattern of their recognition sites. The pattern is designed so that one orientation (corresponding to an ON output) only occurs for the right combinations of input recombinases. The piece of DNA that is inverted contains a promoter (or genes and other regulatory parts) that will only transcribe an output gene when it is in the ON orientation. This architecture has been shown to be able to record multiple stimuli according to the desired logic.

**Received:** September 11, 2015
**Published:** November 9, 2015




DOI: 10.1021/acssynbio.5b00170
*ACS Synth. Biol.* 2015, 4, 1361−1372

However, there is a problem in using this type of system for combinatorial logic, which requires that the circuit continuously respond with the correct logic based on the state of the inputs.[32] When using irreversible recombinases, once the output is in the ON state, it can never return to the OFF state. A similar issue is that the input promoters do not have to be turned on at the same time for the output to respond. For example, the inputs to the AND gate can be ON at different times and never simultaneously and the output will still be ON. To surmount this issue, Endy and co-workers suggested that rewritable logic could be designed by continuously expressing the integrase to hold one state and then one input is connected to the expression of excisionase.[18] In this design, if the input is turned OFF, the output returns to the OFF state. However, one gate requires two genes, one of which is continuously expressed, and this may not be advantageous over other biochemistries used to build NOT gates.[33−37] This is particularly problematic for large circuits that would require the simultaneous expression of many integrases to hold the states of the gates.

In this manuscript, we work with a pair of complementary irreversible recombinases (FimE and HbiF).[5,38−40] When one flips the DNA, this creates the recognition site for the other and vice versa. FimE is a unidirectional recombinase that only has a low affinity for the recognition site after the inversion.[41−43] Another recombinase associated with the *fim* genes is FimB which will return the DNA to the preinversion population. However, it acts bidirectionally and this leads to a mixed population.[44−46] HbiF is encoded in a genomic region unlinked to the fimbriae genes in uropathogenic *E. coli* (it is not present in *E. coli* MG1655) and was discovered by assays to rescue the locked switch when FimB is not present.[39,47,48] It was shown to be specific to the recognition site that occurs after the FimE inversion and it irreversibly catalyzes the transition to the initial state.[29] The advantage of this pair is that a single protein is responsible for each change in memory state.

We have built a set:reset memory switch and a rewritable NOT gate based on the FimE/HbiF recombinases. For the memory switch, two inducible inputs are used to drive the expression of the recombinase. The switch is cycled between set, reset, and hold (no inducer) for >600 h and the function is monitored by a fluorescent reporter and flow cytometry. The circuit breaks at 400 h via an insertion element (IS1) in the pSwitch plasmid. Then, a NOT gate is built where HbiF is constitutively expressed to hold the OFF state and an inducible input promoter is used to drive FimE. This gate is shown to respond transiently to the activity of the input promoter. However, it breaks relatively quickly after only 2 cycles and 54 h of use. Interestingly, the circuit itself is not modified, but rather a mutation of the host strain renders the circuit nonfunctional (*via* insertion elements that disrupt the *pcnB* and *dcuR* genes). Understanding the evolutionary mechanisms that interfere with circuit function will aid the design of more robust versions and will guide the use of classes of regulatory proteins and RNA for different end uses.

## RESULTS

**A Resettable Memory Switch Based on FimE and HbiF.** The memory switch is designed to respond to two inputs and control a third output (Figure 1A). Drawing the borders of the switch at promoters follows the paradigm of using RNA polymerase fluxes as the common signal carrier that facilitates the connection of circuits.[32,49,50] The inputs to the switch are the IPTG ($P_{tac}$) and arabinose ($P_{BAD}$) inducible systems, which drive the expression of HbiF and FimE, respectively. The recognition sites for these DNA invertases are 9-bp inverted repeats (IRL and IRR).[39,42,51] The FimE IRL and IRR sites are AATACAAGACAATTGGGGCCATTTTGACTCATAGAG and ATGATATGGACAGTTTGGCCCCAAATGTTTCATCTTTTG, where the binding site and the 9-bp repeated sequence are underlined. The inversion reaction converts these sequences to $IRL_{hbiF}$ AATACAAGACAATTGGGGCCAAACTGTCCATATCAT and $IRR_{hbiF}$ CTCTATGAGTCAAAATGGCCCCAAATGTTTCATCTTTTG, which correspond to the sites recognized and inverted by HbiF.[39] The constitutive promoter $P_{trc*}$ (lacking lacO sites) is placed between the IRL and IRR sites so that it is only in the proper orientation to transcribe a green fluorescent protein (*gfp*) reporter when the switch is in the SET state. The inverted sequence (344 bp) is located between the $P_{trc*}$ promoter and the *gfp* gene. As observed previously, the maximum induction levels are relatively low, which could be a result of secondary structures forming in the inversion region that negatively impact RBS strength.[13] A two-plasmid system is used where the invertases and inducible systems are carried on a ColE1 backbone (pSwitch) and the recognition sites and reporter are on a p15a backbone (pReporter) (Figure S1, Supporting Information).

The expression levels of HbiF and FimE had to be tuned to obtain a functional circuit. The ribosome binding site (RBS) controlling *fimE* was previously changed as part of connecting it to the arabinose-inducible system.[14] However, initially HbiF expression under the $P_{tac}$ promoter was too strong and led to impaired cell growth after IPTG induction. To reduce HbiF expression, the N-terminal degradation tag YIALR[52] was added to the HbiF coding sequence, which led to a functioning IPTG-inducible HbiF construct. The LtvsJ insulator[37,53] was added before the HbiF RBS.

The memory switch was characterized by measuring the threshold of input required to switch between the two states (Figure 1B). The inputs to the switch are the $P_{BAD}$ and $P_{tac}$ promoters. In order to report the switch properties in terms of promoter activities, as opposed to inducer concentrations, a separate system of reporter plasmids was built and characterized (Supporting Figures S1 and S2).[54] First, the reset → set transition was measured by starting with cells containing the pSwitch and pReporter plasmid in the OFF state and then inducing with different concentrations of IPTG (Supporting Methods). The opposite transition was also tested, where the cells were grown in the presence of the set signal (1 mM IPTG), subjected to an overnight growth cycle in the absence of inducer and then induced with different concentrations of arabinose. Individual cytometry histograms for each data point are shown in Figure S2. Because the invertases are irreversible, we expected the response function to drift over time. However, it quickly converged to a steady-state curve, likely due to a low level of constitutive expression of the opposing invertase (Supporting Figure S2). The response function ($t$ = 8 h) can be fit to

$$Y = Y_{min} + (Y_{max} - Y_{min})\frac{I_x^{\,n}}{K^n + I_x^{\,n}} \quad (1)$$

where $Y_{min}/Y_{max}$ are the min and max fluorescence values of the output, $K$ is the threshold, and $n$ is the Hill coefficient. $I_x$ is the promoter activity of input $x$ in arbitrary units. Eq 1 was fit to


DOI: 10.1021/acssynbio.5b00170
ACS Synth. Biol. 2015, 4, 1361−1372

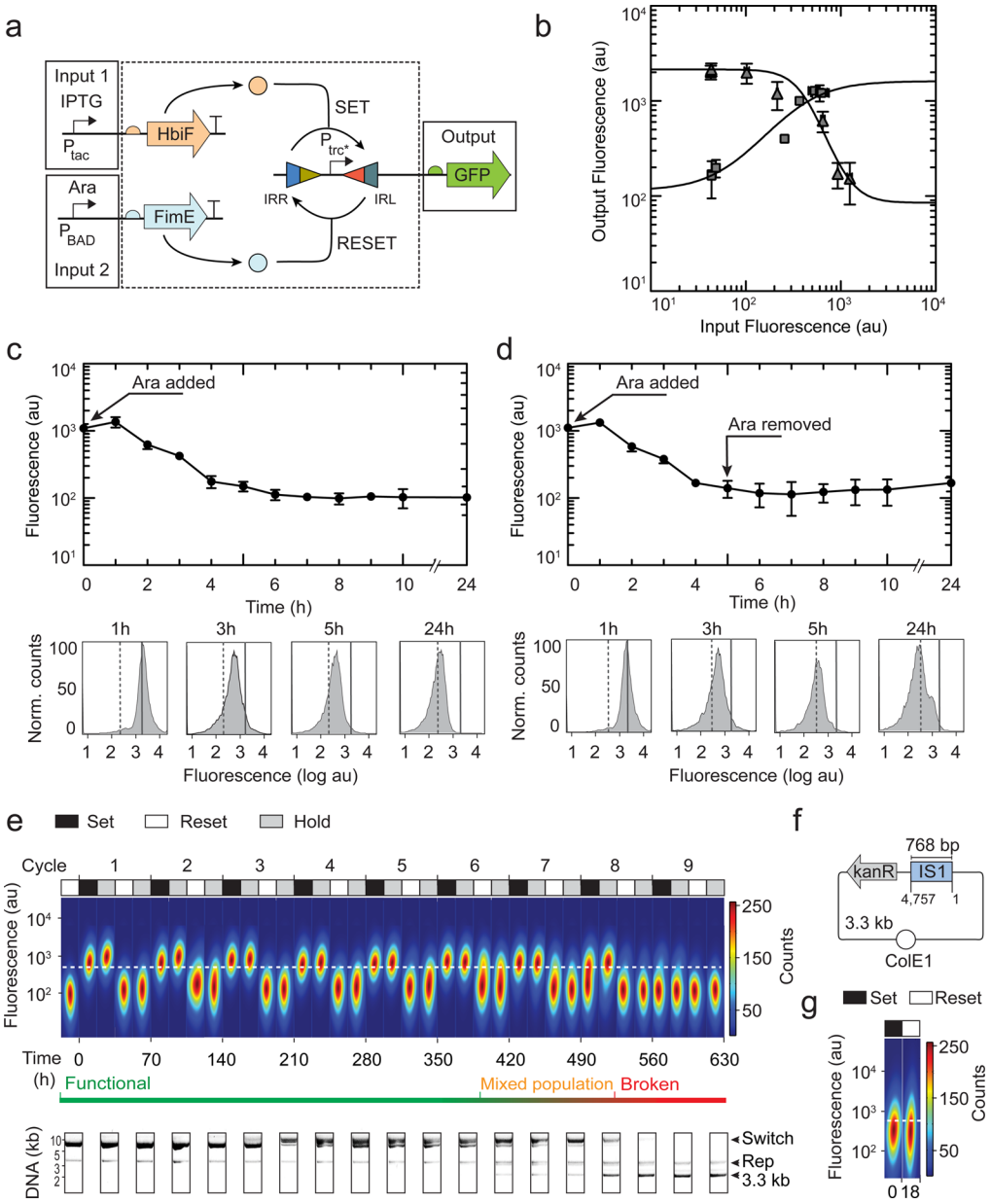


**Figure 1.** The memory switch: dynamics and evolutionary stability. (A) A schematic of the switch is shown. The plasmid map and genetic part sequences are provided in Supporting Figure S1 and Table S1, respectively. $P_{trc*}$ is a constitutive promoter based on a truncated *trc* promoter lacking *lacO* binding sites.[13] (B) The response function of the switch is shown for the set → reset (triangles) and reset → set (squares) transitions. For the set → reset transition, cells are initially grown with the pReporter plasmid in the *on* configuration and then transferred to media with different concentrations of arabinose and grown for 8 h (Supplemental Methods). The *x*-axis is converted from concentration of inducer to fluorescence using a separate plasmid system that measures the activity of the $P_{tac}$ or $P_{BAD}$ promoter (Supporting Figure S2). Black lines show the fit to eq 1, the parameters for which are in Table 1. (C) A time course is shown demonstrating the time required to turn the switch off after the input (1 mM arabinose) is added at $t = 0$ (Supporting Methods). Cytometry data is shown at four time points (solid and dashed lines are the means at 1 and 24 h, respectively). (D) The time course is repeated as in part C except the input is removed at $t = 5$ h by resuspending in fresh medium without inducer. (E) Cells are passaged while being cycled between states. Set, reset, and hold refer to the presence of 1 mM IPTG, 1 mM of arabinose, and the absence of inducers, respectively. Aliquots are taken and analyzed by cytometry; the width of the distributions is RFP used as a gate. The dashed white lines mark the threshold for the ON state. During the time course, DNA was purified from the aliquots and run on an agarose gel that is imaged and inverted (Supporting Methods). "Switch" and "Rep" refer to the expected positions for the pSwitch and pReporter plasmids (7.3 kb and 4.5 kb, respectively). "3.3 kb" shows the emergence of a smaller band over time. (F) The broken plasmid containing the IS1 element (blue) is shown. The numbers correspond to the original 7.3kb plasmid (Figure S1). (G) The broken plasmid was purified and retransformed into fresh *E. coli* DH10b cells containing the pReporter plasmid that were then subjected to a new set-reset cycle. For all parts of this figure, error bars represent the standard deviation of three independent experiments performed on different days.

the data, the parameters for which are shown in Table 1 (Supporting Methods).

A time course was performed to measure the dynamics of switching between states. Starting from the set state, arabinose was added at time 0 and aliquots were taken every hour (Figure 1C). Every 2 h, the cells were passaged to fresh media containing the inducer. The transition began to occur after 2 h and cells were fully reset after 4 h. This transition is graded,



DOI: 10.1021/acssynbio.5b00170
*ACS Synth. Biol.* 2015, 4, 1361−1372

**Table 1. Parameterization of the Memory Switch and NOT Gate Response Functions**

| | parameters (eq 1)[a] | | | |
|---|---|---|---|---|
| name | $K$ (au) | $n$ | $Y_{max}$ (au) | $Y_{min}$ (au) |
| Switch (set → reset) | 340 ± 40 | 2.6 ± 0.3 | 2100 ± 300 | 90 ± 10 |
| Switch (reset → set) | 360 ± 70 | 1.6 ± 0.1 | 1600 ± 100 | 110 ± 30 |
| NOT Gate | 770 ± 10 | 4.5 ± 0.3 | 1300 ± 100 | 120 ± 60 |

[a]Shown as the average and standard deviation of three independent fits to three experiments performed on different days.

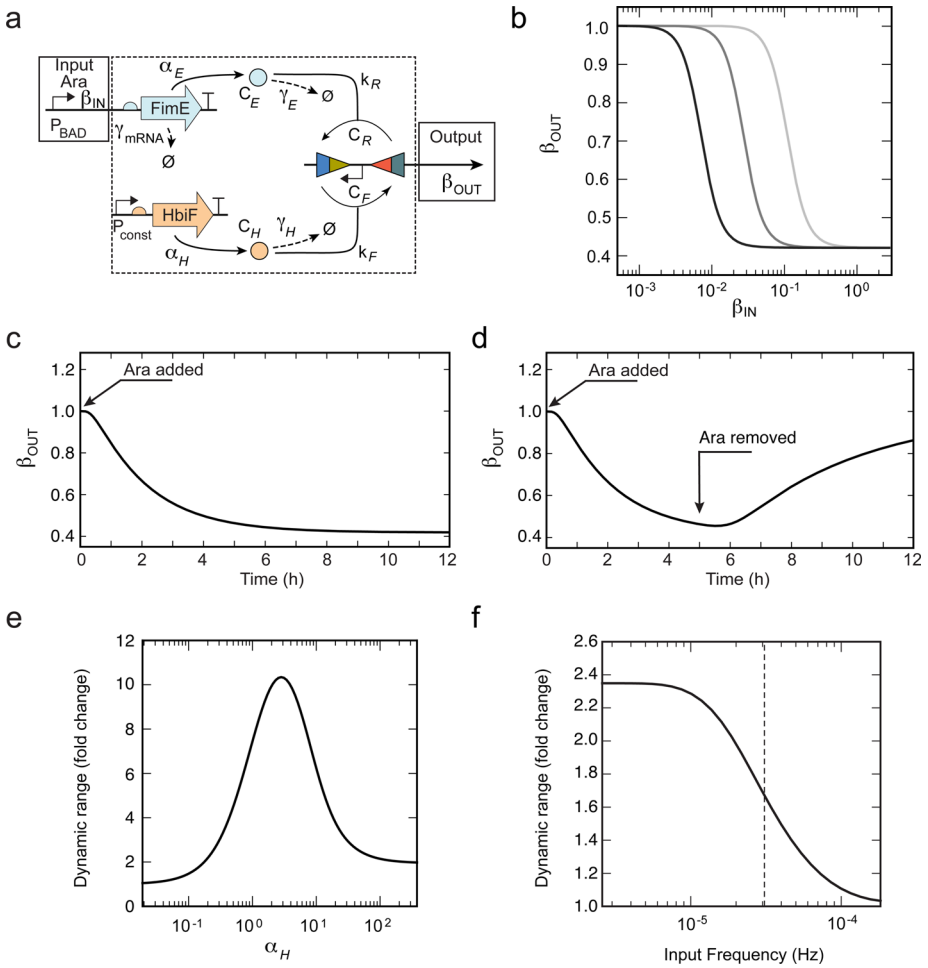


**Figure 2.** Mathematical model of the NOT gate. (A) Illustration showing the model parameters (Table 1). (B) The response function of the NOT gate is shown. From left to right, the curves represent different expression rates of FimE ($\alpha_E$ = 192, 48, 12 proteins per transcript per minute), which show how the threshold could be changed by varying the associated RBS. (C) A time course is shown where the cells are initiated in the set state and arabinose is added at $t$ = 0. (D) The response when arabinose is removed and the cells return to the set state is shown. (E) Influence of HbiF protein production rate $\alpha_H$ on gate performance. For each $\alpha_H$ value the input promoter $\beta_{IN}$ was fully activated and the system was simulated for alternating 48 h ON then 48 h OFF input states for 15 complete cycles. Performance was calculated as the dynamic range (the maximum divided by the minimum output state $\beta_{OUT}$) averaged over the last 5 cycles of the simulation. Autofluorescence of white cells was taken to be equivalent to 0.01 transcripts per minute of the output promoter. (F) Influence of input switching frequency on the dynamic range of the gate. The gate was provided with an alternating fully ON (arabinose present), fully OFF (arabinose absent) input at the specified frequency. The dotted line denotes input frequency of 9 h.

indicating that cells undergo intermediate states in which they contain a mixed population of set and reset pReporter plasmids. The experiment was then repeated, except after the cells were fully reset (5 h) they were washed in fresh media and passaging was continued in the absence of inducer (Figure 1D) (Supporting Methods). After 24 h, there was a slight upshift in the fluorescence, which could be seen as bimodality in the cytometry distribution. This could be due to the leaky expression of the invertases in the absence of inducers, the ratio of which slightly biases toward to the set state. This is a consequence of having both invertases present in the cell, as opposed to one that results in a permanent change in state. There are a number of ways to reduce leaky gene expression and these may help increase the stability of the held states.[55] Unbalanced expression will always lead to drift toward one of the states, leading to a loss in memory.

**Evolutionary Stability of the Memory Switch.** We tested the ability of the memory switch to function as designed over long times. Cells were continuously passaged into fresh media under conditions to set (1 mM IPTG), hold (no



DOI: 10.1021/acssynbio.5b00170
ACS Synth. Biol. 2015, 4, 1361−1372

**Table 2. Model Parameter Values**

| name | description | value | units | ref |
|---|---|---|---|---|
| $\beta_{IN}$ | $P_{BAD}$ transcription rate | 0.05−25[a] | transcript cell$^{-1}$ min$^{-1}$ | 58,110 |
| $\alpha_E$ | Production rate of FimE | 12 | protein transcript$^{-1}$ min$^{-1}$ | 89 |
| $\alpha_H$ | Production rate of HbiF | 60 | protein cell$^{-1}$ min$^{-1}$ | 89 |
| $\gamma_{mRNA}$ | mRNA degradation rate | 5 | min$^{-1}$ | 111 |
| $\gamma_E$ | FimE protein degradation rate | 0.017[b] | min$^{-1}$ | |
| $\gamma_H$ | HbiF protein degradation rate | 0.069 | min$^{-1}$ | 89 |
| $k_R$ | FimE inversion rate constant | $5.78 \times 10^{-3}$ [c] | min$^{-1}$ | 29 |
| $k_F$ | HbiF inversion rate constant | $5.78 \times 10^{-3}$ [c] | min$^{-1}$ | 29 |
| $K_E$ | FimE dissociation constant | 1144[d] | protein cell$^{-1}$ | |
| $K_H$ | HbiF dissociation constant | 478[d] | protein cell$^{-1}$ | |
| $m$ | FimE cooperativity | 3.1[e] | – | |
| $n$ | HbiF cooperativity | 1.4[e] | – | |
| $C_T$ | Total concentration of output promoter | 2.5[f] | promoter cell$^{-1}$ | |
| $\varepsilon$ | $P_{Const}$ transcription rate | 0.4[g] | transcript promoter$^{-1}$ min$^{-1}$ | |

[a]Range is given for that measured in the absence and at saturating concentrations of arabinose. [b]No degradation tag is present so dilution via growth is the dominant mode of degradation. Doubling time of the cells during these experiments was determined to be 40 min. [c]Strongly expressed recombinases have been shown to require between 2 and 6 h to flip the majority of sites in a p15A origin plasmid.[29] Assuming under these conditions that substrate is fully bound, inversion rate is given by $\ln(2)/120 = 5.78 \times 10^{-3}$ per minute. This approximate rate is used for both invertases. [d]$K$'s in Figure 1B are scaled by the maximum steady-state concentrations (e.g., $\alpha_H/\gamma_H$) in order to obtain units of concentration. [e]Estimated from FimE and HbiF response functions (Figure 1B). [f]Determined by experiments (Figure 3J). [g]Chosen to ensure a maximal output transcription rate $\beta_{OUT}$ = 1 transcript per minute.

inducer), and reset (1 mM arabinose) the switch (Supporting Methods). The switch was tested by cycling between the set-hold-reset-hold conditions for almost a month (>600 h) (Figure 1E). Each cycle of four steps was performed over a 70-h period. At the end of each step, an aliquot of cells was taken and the fluorescence measured by flow cytometry. In addition, the plasmids were extracted and run on a DNA gel to look for any genetic modifications to the circuit.

The circuit responded uniformly as designed over 6 cycles (>400 h, 17 days). During this period, there was no loss of performance, reduction in dynamic range, or increase in population variability. In addition, the two-plasmid system was recovered without additional bands. However, during the reset step of the sixth cycle, a bimodal population appeared, where a fraction of the cells remained ON when they should have switched OFF. When the circuit was cycled back to the ON state, the population again appeared uniform, but in the reset phase it was bimodal and the circuit eventually completely broke by cycle 9. This behavior was reflected in the DNA gel where after the sixth cycle, the bimodal distribution coincided with the appearance of a smaller band that was enriched in each subsequent cycle. The band corresponding to the pSwitch plasmid weakened and eventually disappeared.

DNA sequencing revealed that the smaller band contained the origin of replication *ColE1*, the kanamycin resistance gene and a 768-bp novel sequence replacing the *araC*, *fimE*, *lacI* and *hbiF* genes (Figure 1F). A BLASTN analysis revealed that the 768-bp sequence corresponded to mobile element *IS1*. The insertion regions were AT rich (GC content ∼25% and ∼37% respectively), which agrees with previous observations that *IS1* prefers to target AT rich sequences.[56] A gain of fitness likely occurred because the recombined plasmid did not express the invertases and this eventually overtook the population. The loss of function of the recombined plasmid was confirmed by transforming it into cells harboring the pReporter plasmid, as shown in Figure 1G. As expected, cells carrying the recombined IS1-containing plasmid were not able to switch the circuit on in the presence of IPTG.

**Model-Based Design of a Rewritable NOT Gate.** A NOT gate is a one-input one-output logic function, where the output is held in the opposite state as the input. The input to the gate is a promoter, which drives the expression of one invertase so that the switch flips to the ON state (Figure 2A).[18] The second invertase is constitutively expressed and holds the gate in the OFF state when the input promoter is not active. Therefore, the output will only be OFF when the input promoter is ON and when it turns OFF the gate will transiently return to its original state. For this design to work, the induced invertase must be able to outcompete the constitutively expressed one to obtain a steady state that is uniform across the population. Because the input and output are promoters, the gate is as easy to layer as designs based on repressors and CRISPRi.[37,57] The gate can be converted to a multi-input NOR gate by connecting multiple input promoter in series.[58]

It is important that expression levels of the invertases are tuned such that competition between them maximizes the dynamic range between ON and OFF states. A mathematical model was derived to quantify this effect for the HbiF/FimE NOT gate. The input to the gate is the transcription rate $\beta_{IN}$ from the input promoter. The dynamics of the gate can be captured by two differential equations that track the concentration of FimE $C_E$ and the concentration of promoters that are in the set state $C_F$:

$$\frac{dC_E}{dt} = \left(\frac{\beta_{IN}}{\gamma_{mRNA}}\right)\alpha_E - \gamma_E C_E \tag{2}$$

and

$$\frac{dC_F}{dt} = k_F(C_T - C_F)\left(\frac{C_H{}^n}{K_H{}^n + C_H{}^n}\right) - k_R C_F\left(\frac{C_E{}^m}{K_E{}^m + C_E{}^m}\right) \tag{3}$$

The concentration of HbiF $C_H = \alpha_H/\gamma_H$ is assumed to be at quasi-steady state and output of the gate $\beta_{OUT} = \varepsilon C_F$, where $\varepsilon$ is the transcription rate from the constitutive promoter. We also assumed a fixed concentration of output promoter $C_T = C_F +$



DOI: 10.1021/acssynbio.5b00170
ACS Synth. Biol. 2015, 4, 1361−1372

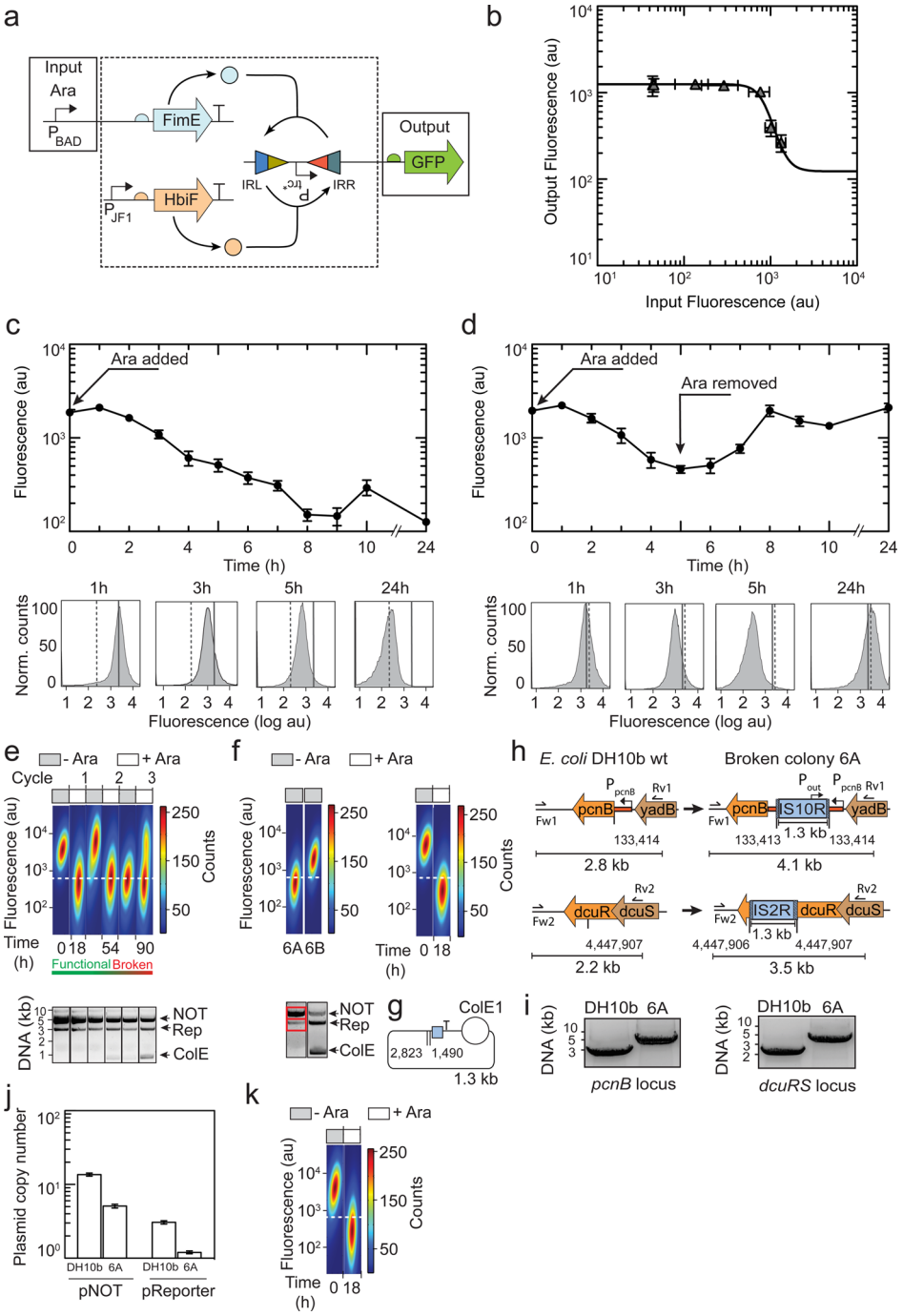


**Figure 3.** The NOT gate: dynamics and evolutionary stability. (A) A schematic of the combinatorial NOT gate is shown. The symbols and sequences correspond to Figure 1A. Plasmid maps and genetic part sequences are provided in Supporting Figure S1 and Table S1. (B) The response function is shown for FimE expressed to different levels by adding arabinose in the presence of constitutively expressed HbiF. The cells are grown in the presence of inducer for 8 h, analyzed by flow cytometry and fit to eq 1. The *x*-axis is converted from mM arabinose to $P_{BAD}$ activity using a separate reporter system (Supporting Figure S2). (C) A time course is shown demonstrating the time required to turn the switch off after the input (1 mM arabinose) is added at $t = 0$ (Supporting Methods). Cytometry data is shown at four time points (solid and dashed lines are the means at 1 and 24 h, respectively). (D) The time course is repeated as in part C except the input is removed at $t = 5$ h by resuspending in fresh medium without inducer. (E) A time course is shown following the same format described in Figure 1E. Cells are cycled between media with and without arabinose (1 mM) in 18-h periods. After each growth period, aliquots are taken and plasmid DNA is purified and run on an agarose gel (Supporting Methods). "NOT" and "Rep" refer to the expected positions for the pNOT and pReporter plasmids (7.3 kb and 4.5 kb, respectively). "ColE1" shows the emergence of a smaller band that corresponds to a plasmid containing only the origin of replication, confirmed by sequencing. (F) The culture at the end of the third cycle was streaked onto an LB agar plate and single colonies selected, regrown, and analyzed by cytometry to identify different subpopulations 6A and 6B (high and low fluorescence levels, top left panels). Aliquots were taken and DNA was purified and analyzed as in part E (bottom left panels). The invertase and reporter plasmids were purified from colony 6A (red boxes), retransformed into fresh *E. coli* DH10b cells, and subjected to a new cycle (top right panels). (G) The sequenced 1.3kb plasmid is shown. The blue box depicts a single 60-bp sequence that appeared twice in the original pNOT plasmid flanking the regions 1490 and 2823. (H) Genomic DNA from wild-type *E. coli* DH10b cells and colony 6A was isolated and sequenced. The locations in which the IS2R and ISR10R mobile elements insert are shown. The numbering corresponds with


DOI: 10.1021/acssynbio.5b00170
*ACS Synth. Biol.* 2015, 4, 1361−1372

**Figure** 3. continued

the *E. coli* DH10b genome (GenBank accession CP000948.1). The red box shows the promoter region of *pcnB*[108] that is disrupted by the IS10R element. The shaded gray boxes denote the repeated flanking sequence GCCAT for IS2R and AGCTCAGCA for IS10R. The internal promoter in IS10R is shown ($P_{out}$). The expected band sizes that would result from PCR using the forward (Fw1, internal to the *yadB* region upstream of *pcnB* and Fw2, internal to *dcuS*) and reverse (Rv1, downstream of *pcnB* and Rv2, internal to *dcuB*) primers are shown at the bottom of each image. (I) The results of PCR amplification of the genomic regions in part D using the primer sets (Fw1/Rv1) and (Fw2/Rv2) are shown. (J) The copy numbers of the pNOT and pReporter plasmids are calculated using qPCR when carried in *E. coli* DH10b cells (WT) and the strain isolated from colony 6A. The qPCR data was converted to copy number using a previously published method (Supporting Methods) by comparing the number of copies of the kanamycin and chloramphenicol resistance genes (encoded in pNOT and pReporter, respectively) to the number of copies of the *dxs* gene (one copy per genome).[109] Error bars represent the error of three qPCR quantifications from samples grown on different days. (K) The strain corresponding to colony 6A, which is already carrying the pNOT and pReporter plasmids, was transformed with a BAC constitutively expressing wild-type *pcnB* (ppcnB, Supporting Information). This strain was subjected to a cycle of induction, as in part E.

$C_R$. The model parameters were estimated based on characterization data for each invertase (Figure 1) and the literature (Table 2). Using Equations 2 and 3, the performance of the gate was simulated (Methods). The response functions (Figure 2B) and dynamic behavior (Figure 2C and Figure 2D) are consistent with those observed experimentally.

Using the model, we calculated the maximum dynamic range (fold change) between the ON and OFF states that can be achieved by balancing the expression levels of HbiF and FimE. Keeping the protein production rate of FimE $\alpha_E$ fixed, we varied the production rate of HbiF $\alpha_H$ and analyzed the impact on the observed dynamic range. If $\alpha_H$ is high, then FimE cannot sufficiently overcome HbiF to turn the switch OFF and if it is too low, then the switch is always OFF. An optimal range was achieved for $\alpha_H \approx 2.9$ proteins per minute, with the dynamic range decreasing for smaller and larger values (Figure 2E). The frequency response was also measured (Figure 2F). This predicts that the input needs to be sustained in the ON or OFF state for >4.5 h to achieve >50% of the maximum dynamic range.

**Construction of a Rewritable NOT Gate Using FimE and HbiF.** The NOT gate was constructed by modifying the genetic system used to characterize the memory switch (Figure 3A). The promoter that serves as the input to the gate ($P_{BAD}$) is used to express FimE, which drives the switch to the OFF state. HbiF is constitutively expressed to maintain the gate in the ON state when $P_{BAD}$ is inactive. Different concentrations of HbiF were tested by using a library of constitutive promoters[59] (Supporting Methods). The library was screened by selecting 26 random single colonies and evaluating their expression in the absence and presence of 1 mM arabinose. Of these, 23 showed no fluorescence in either condition, indicating that HbiF expression is too low. One had intermediate levels of fluorescence in both conditions. Two behaved as expected, with *gfp* expressed only in the absence of inducer. One was sequence-verified and selected for subsequent analysis (Supporting Figure S3). The constitutive promoter was designated $P_{JF1}$ and the plasmid referred to as pNOT (Supporting Figure S1).

The response function (Figure 3B) and temporal dynamics (Figure 3C) of the NOT gate were then evaluated. As with the memory switch, there was a 2 h lag before the initial response was observed and the gate was not fully OFF until 8 h after the addition of 1 mM arabinose. This took longer than the memory switch, as would be expected because the background concentration of HbiF needs to be overcome. The response function was evaluated for different concentrations of arabinose at 8 h (Figure 3B). They were fit to eq 1 and the resulting parameters are shown in Table 1. The function was more digital than the memory switch, with a higher threshold and OFF state. These changes are all consistent with the need to overcome HbiF, which has a similar effect as other thresholding mechanisms.[60−62] Individual histograms for different concentrations of arabinose are shown in Supporting Figure S2.

A time course was performed to demonstrate the resetting of the NOT gate when the input promoter turned off. The same experiments were performed as described for the memory switch (Supporting Methods). When the cells were passaged with 1 mM inducer, the gate turned OFF and this was stable so long as the inducer was present (Figure 3C). However, when they were put in media lacking the inducer at $t$ = 5 h, the switch reverted to the initial ON state (Figure 3D). The time scale to fully transition back to the ON state was faster, requiring 3 h to complete. The transition was graded in both directions and the cell populations were indistinguishable before or after the cycle.

**Evolutionary Stability of the NOT Gate.** Cells were passaged while cycling the circuit state, as was done for the memory switch. Each cycle consisted of growing cells in the absence and presence of inducer (1 mM arabinose) for 18 h steps. As before, cells were continuously passaged into fresh media (Supporting Methods). The circuit functioned properly for up to 54 h, after which the circuit broke and was unable to return to the ON state (Figure 3E). At $t$ = 90 h, a bimodal population emerged that was representative of cells in both the ON and OFF state. After each step of a cycle, plasmid DNA was purified and run on an agarose gel. Starting at 54 h, a slight ∼1 kb band began to appear and became more dominant over time. Even after 90 h, the plasmids containing the invertases and reporter were still present.

To further investigate the cause of breakage, cells from the bimodal population were plated and colonies were selected that were representative of low (clone 6A) and high (clone 6B) GFP intensities (Figure 3F). The 6A clone showed only two plasmids, both of which were sequenced to confirm that they were unmutated (Supporting Methods) and corresponded to intact pNOT and pReporter. Conversely, the 6B clone was shown to have less intact pNOT plasmid, relative to which there were high concentrations of the small 1kb band. Neither the pNOT or pReporter plasmids contained mutations, but the 1 kb band corresponded to a ColE1 origin with no resistance marker (Figure 3G). The original invertase plasmid contained two identical 60 bp sequences that appeared after the kanamycin resistance gene and again downstream of the ColE1 origin. This suggests a homologous recombination event, which has been frequently observed when passaging genetic circuits.[63−65] Interestingly, both the recombined and original plasmids were maintained in individual cells, which



DOI: 10.1021/acssynbio.5b00170
*ACS Synth. Biol.* 2015, 4, 1361−1372

may be a mechanism of maintaining antibiotic resistance while effectively decreasing copy number.

We were intrigued that clone 6A appeared to be broken despite having both unmutated plasmids. Further, when the plasmids were purified and retransformed into fresh *E. coli* DH10b cells, they functioned normally (Figure 3F). This suggests that clone 6A broke due to a mutation in the host genome. To determine how this occurred, we isolated and sequenced the genomic DNA (Supporting Methods). This revealed that there were two mobile element insertions not present in wild-type *E. coli* DH10b (Figure 3H).

The first event corresponded to the insertion of the 1.3-kb *IS10R* mobile element[66] into the promoter region of the *pcnB* gene (Figure 3H), which was confirmed *via* PCR amplification. This gene encodes a poly(A)-polymerase that is known to be involved in ColE1 origin of replication control.[67,68] When it is disrupted, this leads to lower plasmid copy numbers.[69] The insertion disrupts the *pcnB* promoter and the transposon contains an internal constitutive promoter that runs antisense,[70] which may contribute to the lower promoter activity.[71] A qPCR assay was used to quantify the impact of the disruption on plasmid copy number (Supporting Methods). This resulted in an approximately 3-fold reduction in the copy numbers of both the invertase and reporter plasmids (Figure 3I). This agreed with the sequencing data, where the copy number estimated from the read depths corresponded to 7 copies of the pNOT plasmid and 1.3 copies of the pReporter plasmid (Supporting Methods). Finally, we sought to determine whether the circuit function could be recovered by transforming an additional copy of the *pcnB* gene. The gene and its native promoter were cloned into a BAC and transformed into broken clone 6A (maintaining the pNOT and pReporter plasmids already there). As shown in Figure 3J, this recovered circuit function, thus indicating that this is the primary cause of the failure.

The second event corresponded to an insertion of the 1.3-kb transposon *IS2R*[72] within the genomic locus of *dcuRS* (Figure 3D), confirmed by PCR amplification (Figure 3H). These genes encode a two-component system involved in C4-dicarboxylate sensing and utilization.[73] Three additional SNPs were also detected in colony 6A (Supporting Methods). It is unclear whether these provide additional gain-of-fitness and they may be reflective of neutral evolutionary drift and stress-induced transposon activity.[74−79]

## DISCUSSION

A variety of biochemical mechanisms have been used to implement memory and combinatorial logic in cells.[18,31,57,80−82] Invertases have the advantage that their state is defined by a discrete structure of DNA. In terms of memory, because the state is not defined by concentrations of protein or mRNA, the state is held until it is accessed, which can occur after the cell dies. It also does not require continued expression for maintenance of the state. For combinatorial logic, it offers the advantage of having an equivalent discrete state to represent 0 and 1, as opposed to architectures where these are defined as the absence or presence of a biomolecule. Here, we harness two invertases (FimE and HbiF) that are encoded by single genes that irreversibly flip a unit of DNA in opposing directions. We demonstrate that these proteins can be used to build a resettable memory switch and NOT gate.

Transcriptional gates, where the inputs and outputs are promoters, are simple to layer to build larger circuits. Following this paradigm, transcriptional NOT and NOR gates have been found to be versatile as an elemental computational operation from which dynamic and multi-input multioutput circuits can be constructed. The NOT gate function requires molecular biology that can implement repression. The simplest is a single repressor protein that, when expressed, turns off the output promoter. There are also RNA-based mechanisms, including CRISPRi and toehold RNA,[82−84] which can perform this function. These potentially enable the scale-up to circuits composed of many gates because it is relatively easy to engineer orthogonal sets of regulators and the amount of DNA required to encode a gate is small (~200 bp).[37] It is not clear what advantage the invertase-based resettable NOT gate has over these designs. It requires two genes, one of which must be constitutively expressed, and 1.8kb to implement. The kinetics, dynamic range, and cooperativity are roughly equivalent. Further, the model and experiments show that the primary advantage of using invertases—that they can hold a state—is lost when circuits involve the expression of opposing invertases. Leakiness or an expression misbalance can easily cause the circuit to drift from holding a state.

Many of the genetic circuits developed to date have not been tested for evolutionary stability. In most cases, there are at least some toxic components. For example, some protein repressors can be toxic when overexpressed.[57,62,85] For CRISPRi circuits, the sgRNAs are not toxic, but Cas9 is in many organisms. One of the challenges is that the function of genetic circuits is defined by many states: for logic, each combination of inputs results in a different combination of regulators being expressed and this is continuously changing for dynamic circuits. Because the burden is a function of regulator expression, the evolutionary stability depends on the state in which the circuit is carried. This is shown by Endy and co-workers where they note that a quorum sensing circuit is carried over many generations in the OFF state, but breaks quickly when carried in the ON state.[65] The source of the evolutionary instability is often unclear, even in knowing whether it is due to toxicity specific to a regulator (or off-target expression) or metabolic/load burden, and this complicates rationally engineering stability into a circuit. Instead, the approach has largely been to engineer circuits (or more broadly, genetic devices) to be more robust to mechanisms of evolutionary mutagenesis[32,86−88]

The memory switch and NOT gate both break when passaged over long times and the function of the circuit is cycled. Note that, while this occurs much more quickly than the memory switch, the total time over which integrases are expressed is similar. In the memory switch, the invertases are expressed for 210 h (12 periods of 17.5 h) before breaking. For the resettable NOT gate, one invertase is expressed for 72 h and two invertases are expressed simultaneously for 72 h. If one assumes that evolutionary pressure combines linearly when multiple proteins are expressed, then the total pressure on the cells is nearly identical for the length of these experiments before the circuits break.

The three cases of breakage that we evaluate reveal three different mechanisms by which the circuits are inactivated. Homologous recombination is probably the most frequent culprit in disrupting circuits.[63−65] The designers of early circuits lacked high-quality parts with sufficient sequence diversity, and the reuse of parts such as promoters and terminators has been historically problematic.[63,65,89] With the increase in large part libraries,[64,90,91] this can now be easily avoided. The other mechanisms involve transposable insertion elements. In some cases the same evolutionary solution involving insertion


DOI: 10.1021/acssynbio.5b00170
ACS Synth. Biol. 2015, 4, 1361−1372

elements appears in independent experiments.[92] Here, we observe disparate disruption mechanisms enacted by different insertion elements. In one, the circuit components are eliminated from the pSwitch plasmid by IS1 insertion. In the second one, the circuit itself is disrupted in a manner that maintains antibiotic resistance by carrying multiple forms of the plasmid in single cells whereas in the other the genome is modified to reduce copy number. Both of the latter mechanisms were difficult to debug, where simple PCR assays to test for an element or retransformation of the plasmids in fresh cells would imply the presence of functional circuits.

When designing a circuit to be stable, it is important to consider the specifications required by the end application. For example, circuits do not need to be robust for months if designed for a one-week fermentation. Design principles can be combined to build circuits for applications that require long-term stability. These include (1) elimination of repeated part sequences above ∼25 bp, (2) reduction of recombinant expression levels,[63,89,93−96] (3) incorporation of redundant regulatory mechanisms,[86,97] and (4) avoidance of constitutive expression. Buffering against insertion elements is a more daunting challenge. Using strains where these have been deleted from the genome[98,99] may seem like an obvious choice, but most applications require using more robust wild strains or difficult-to-manipulate species and insertion elements are very common across all kingdoms of life.[100] Exacerbating this challenge is that many of these elements are induced by the stresses imposed by carrying a foreign circuit.[101] Multiplexed genome editing may provide a mechanism to rapidly eliminate the elements from new, wild strains.[102−106] Placing the circuit in the genome could also improve stability, as this is a common approach to improve the robustness of strains in metabolic engineering. However, this is a more complex problem for circuits, where regulator expression is more difficult to control in the genome and carrying a multiregulator circuit may evoke evolutionary pressure that makes strain maintenance more difficult. Measuring the evolutionary failure modes of circuits, mechanisms to engineer counters to these failures, and the assignment of appropriate molecular biology to different circuit functions, will lead to a new generation of evolutionarily robust circuits.

## ■ ASSOCIATED CONTENT

### Supporting Information

The Supporting Information is available free of charge on the ACS Publications website at DOI: 10.1021/acssynbio.5b00170.

Table S1: Genetic parts used in this study. Table S2: Transposon sequences identified. Figure S1: Plasmid maps. Figure S2: Representative histograms used to build the response functions. Supporting Methods. Figure S3: Constitutive promoter screen. Supporting References. (PDF)

## ■ AUTHOR INFORMATION


### Corresponding Author

*E-mail: cavoigt@gmail.com.


### Author Contributions

C.A.V, J.F.R. and L.Y. conceived of the study and designed the experiments. J.F.R. and L.Y. performed the experiments and analyzed the data. D.B.G. performed the genomic analysis. T.E.G. developed the ODE model. C.A.V., J.F.R, D.B.G, T.E.G and L.Y. wrote the manuscript.

### Notes

The authors declare no competing financial interest.

## ■ ACKNOWLEDGMENTS

This work was supported by US National Science Foundation Synthetic Biology Engineering Research Center (SynBERC EEC0540879), the US Defense Advanced Research Projects Agency (DARPA CLIO N66001-12-C-4016), and the Office of Naval Research Multidisciplinary University Research Initiative (N00014-11-1-0725).

## ■ REFERENCES


(1) Sternberg, N., and Hamilton, D. (1981) Bacteriophage P1 site-specific recombination. I. Recombination between loxP sites. *J. Mol. Biol. 150*, 467−486.

(2) Kunkel, B., Losick, R., and Stragier, P. (1990) The Bacillus subtilis gene for the development transcription factor sigma K is generated by excision of a dispensable DNA element containing a sporulation recombinase gene. *Genes Dev. 4*, 525−535.

(3) Carrasco, C. D., and Golden, J. W. (1995) Two heterocyst-specific DNA rearrangements of nif operons in Anabaena cylindrica and Nostoc sp. strain Mac. *Microbiology 141*, 2479−2487.

(4) Klemm, P., Jørgensen, B. J., Die, I., van Ree, H., and de Bergmans, H. (1985) The fim genes responsible for synthesis of type 1 fimbriae in Escherichia coli, cloning and genetic organization. *Mol. Gen. Genet. 199*, 410−414.

(5) Abraham, J. M., Freitag, C. S., Clements, J. R., and Eisenstein, B. I. (1985) An invertible element of DNA controls phase variation of type 1 fimbriae of Escherichia coli. *Proc. Natl. Acad. Sci. U. S. A. 82*, 5724−5727.

(6) Grindley, N. D. F., Whiteson, K. L., and Rice, P. A. (2006) Mechanisms of Site-Specific Recombination*. *Annu. Rev. Biochem. 75*, 567−605.

(7) Johnson, R. C., and Simon, M. I. (1985) Hin-mediated site-specific recombination requires two 26 bp recombination sites and a 60 bp recombinational enhancer. *Cell 41*, 781−791.

(8) Dybvig, K., and Yu, H. (1994) Regulation of a restriction and modification system via DNA inversion in Mycoplasma pulmonis. *Mol. Microbiol. 12*, 547−560.

(9) Lenich, A. G., and Glasgow, A. C. (1994) Amino acid sequence homology between Piv, an essential protein in site-specific DNA inversion in Moraxella lacunata, and transposases of an unusual family of insertion elements. *J. Bacteriol. 176*, 4160−4164.

(10) Dworkin, J., and Blaser, M. J. (1996) Generation of Campylobacter fetus S-layer protein diversity utilizes a single promoter on an invertible DNA segment. *Mol. Microbiol. 19*, 1241−1253.

(11) Zhao, H., Li, X., Johnson, D. E., Blomfield, I., and Mobley, H. L. (1997) In vivo phase variation of MR/P fimbrial gene expression in Proteus mirabilis infecting the urinary tract. *Mol. Microbiol. 23*, 1009−1019.

(12) Weinacht, K. G., Roche, H., Krinos, C. M., Coyne, M. J., Parkhill, J., and Comstock, L. E. (2004) Tyrosine site-specific recombinases mediate DNA inversions affecting the expression of outer surface proteins of Bacteroides fragilis. *Mol. Microbiol. 53*, 1319−1330.

(13) Ham, T. S., Lee, S. K., Keasling, J. D., and Arkin, A. P. (2006) A tightly regulated inducible expression system utilizing the fim inversion recombination switch. *Biotechnol. Bioeng. 94*, 1−4.

(14) Moon, T. S., Clarke, E. J., Groban, E. S., Tamsir, A., Clark, R. M., Eames, M., Kortemme, T., and Voigt, C. A. (2011) Construction of a genetic multiplexer to toggle between chemosensory pathways in Escherichia coli. *J. Mol. Biol. 406*, 215−227.

(15) Friedland, A. E., Lu, T. K., Wang, X., Shi, D., Church, G., and Collins, J. J. (2009) Synthetic Gene Networks That Count. *Science 324*, 1199−1202.

(16) Baumgardner, J., Acker, K., Adefuye, O., Crowley, S. T., DeLoache, W., Dickson, J. O., Heard, L., Martens, A. T., Morton, N., Ritter, M., Shoecraft, A., Treece, J., Unzicker, M., Valencia, A., Waters,




DOI: 10.1021/acssynbio.5b00170
*ACS Synth. Biol.* 2015, 4, 1361−1372

M., Campbell, A. M., Heyer, L. J., Poet, J. L., and Eckdahl, T. T. (2009) Solving a Hamiltonian Path Problem with a bacterial computer. *J. Biol. Eng. 3*, 11.
(17) Haynes, K. A., Broderick, M. L., Brown, A. D., Butner, T. L., Dickson, J. O., Harden, W. L., Heard, L. H., Jessen, E. L., Malloy, K. J., Ogden, B. J., Rosemond, S., Simpson, S., Zwack, E., Campbell, A. M., Eckdahl, T. T., Heyer, L. J., and Poet, J. L. (2008) Engineering bacteria to solve the Burnt Pancake Problem. *J. Biol. Eng. 2*, 8.
(18) Bonnet, J., Yin, P., Ortiz, M. E., Subsoontorn, P., and Endy, D. (2013) Amplifying Genetic Logic Gates. *Science 340*, 599−603.
(19) Archer, E. J., Robinson, A. B., and Süel, G. M. (2012) Engineered E. coli That Detect and Respond to Gut Inflammation through Nitric Oxide Sensing. *ACS Synth. Biol. 1*, 451−457.
(20) Mimee, M., Tucker, A. C., Voigt, C. A., and Lu, T. K. (2015) Programming a Human Commensal Bacterium, Bacteroides thetaiotaomicron, to Sense and Respond to Stimuli in the Murine Gut Microbiota. *Cell Syst. 1*, 62−71.
(21) Piepenburg, O., Williams, C. H., Stemple, D. L., and Armes, N. A. (2006) DNA Detection Using Recombination Proteins. *PLoS Biol. 4*, e204.
(22) Krõlov, K., Frolova, J., Tudoran, O., Suhorutsenko, J., Lehto, T., Sibul, H., Mäger, I., Laanpere, M., Tulp, I., and Langel, Ü. (2014) Sensitive and Rapid Detection of Chlamydia trachomatis by Recombinase Polymerase Amplification Directly from Urine Samples. *J. Mol. Diagn. 16*, 127−135.
(23) Yamanishi, M., and Matsuyama, T. (2012) A Modified Cre-lox Genetic Switch To Dynamically Control Metabolic Flow in Saccharomyces cerevisiae. *ACS Synth. Biol. 1*, 172−180.
(24) Araki, H., Jearnpipatkul, A., Tatsumi, H., Sakurai, T., Ushio, K., Muta, T., and Oshima, Y. (1985) Molecular and functional organization of yeast plasmid pSR1. *J. Mol. Biol. 182*, 191−203.
(25) McLeod, M., Craft, S., and Broach, J. R. (1986) Identification of the crossover site during FLP-mediated recombination in the Saccharomyces cerevisiae plasmid 2 microns circle. *Mol. Cell. Biol. 6*, 3357−3367.
(26) Thorpe, H. M., Wilson, S. E., and Smith, M. C. (2000) Control of directionality in the site-specific recombination system of the Streptomyces phage phiC31. *Mol. Microbiol. 38*, 232−241.
(27) Ghosh, P., Wasil, L. R., and Hatfull, G. F. (2006) Control of phage Bxb1 excision by a novel recombination directionality factor. *PLoS Biol. 4*, e186.
(28) Brown, W. R. A., Lee, N. C. O., Xu, Z., and Smith, M. C. M. (2011) Serine recombinases as tools for genome engineering. *Methods 53*, 372−379.
(29) Yang, L., Nielsen, A. A. K., Fernandez-Rodriguez, J., McClune, C. J., Laub, M. T., Lu, T. K., and Voigt, C. A. (2014) Permanent genetic memory with > 1-byte capacity. *Nat. Methods 11*, 1261−1266.
(30) Bonnet, J., Subsoontorn, P., and Endy, D. (2012) Rewritable digital data storage in live cells via engineered control of recombination directionality. *Proc. Natl. Acad. Sci. U. S. A. 109*, 8884−8889.
(31) Siuti, P., Yazbek, J., and Lu, T. K. (2013) Synthetic circuits integrating logic and memory in living cells. *Nat. Biotechnol. 31*, 448−452.
(32) Brophy, J. A. N., and Voigt, C. A. (2014) Principles of genetic circuit design. *Nat. Methods 11*, 508−520.
(33) Yokobayashi, Y., Weiss, R., and Arnold, F. H. (2002) Directed evolution of a genetic circuit. *Proc. Natl. Acad. Sci. U. S. A. 99*, 16587−16591.
(34) Lucks, J. B., Qi, L., Mutalik, V. K., Wang, D., and Arkin, A. P. (2011) Versatile RNA-sensing transcriptional regulators for engineering genetic networks. *Proc. Natl. Acad. Sci. U. S. A. 108*, 8617−8622.
(35) Liu, C. C., Qi, L., Lucks, J. B., Segall-Shapiro, T. H., Wang, D., Mutalik, V. K., and Arkin, A. P. (2012) An adaptor from translational to transcriptional control enables predictable assembly of complex regulation. *Nat. Methods 9*, 1088−1094.
(36) Qi, L. S., Larson, M. H., Gilbert, L. A., Doudna, J. A., Weissman, J. S., Arkin, A. P., and Lim, W. A. (2013) Repurposing CRISPR as an RNA-Guided Platform for Sequence-Specific Control of Gene Expression. *Cell 152*, 1173−1183.
(37) Nielsen, A. A., and Voigt, C. A. (2014) Multi-input CRISPR/Cas genetic circuits that interface host regulatory networks. *Mol. Syst. Biol. 10*, 763.
(38) Klemm, P. (1986) Two regulatory fim genes, fimB and fimE, control the phase variation of type 1 fimbriae in Escherichia coli. *EMBO J. 5*, 1389−1393.
(39) Xie, Y., Yao, Y., Kolisnychenko, V., Teng, C.-H., and Kim, K. S. (2006) HbiF Regulates Type 1 Fimbriation Independently of FimB and FimE. *Infect. Immun. 74*, 4039−4047.
(40) iGEM Michigan Synthetic Biology Team. (2012) http://2012.igem.org/Team:Michigan/Project.
(41) Gally, D. L., Leathart, J., and Blomfield, I. C. (1996) Interaction of FimB and FimE with the fim switch that controls the phase variation of type 1 fimbriae in Escherichia coli K-12. *Mol. Microbiol. 21*, 725−738.
(42) Kulasekara, H. D., and Blomfield, I. C. (1999) The molecular basis for the specificity of fimE in the phase variation of type 1 fimbriae of Escherichia coli K-12. *Mol. Microbiol. 31*, 1171−1181.
(43) Holden, N., Blomfield, I. C., Uhlin, B.-E., Totsika, M., Kulasekara, D. H., and Gally, D. L. (2007) Comparative analysis of FimB and FimE recombinase activity. *Microbiology 153*, 4138−4149.
(44) McClain, M. S., Blomfield, I. C., Eberhardt, K. J., and Eisenstein, B. I. (1993) Inversion-independent phase variation of type 1 fimbriae in Escherichia coli. *J. Bacteriol. 175*, 4335−4344.
(45) Gally, D. L., Rucker, T. J., and Blomfield, I. C. (1994) The leucine-responsive regulatory protein binds to the fim switch to control phase variation of type 1 fimbrial expression in Escherichia coli K-12. *J. Bacteriol. 176*, 5665−5672.
(46) Kuwahara, H., Myers, C. J., and Samoilov, M. S. (2010) Temperature Control of Fimbriation Circuit Switch in Uropathogenic Escherichia coli: Quantitative Analysis via Automated Model Abstraction. *PLoS Comput. Biol. 6*, e1000723.
(47) Bryan, A., Roesch, P., Davis, L., Moritz, R., Pellett, S., and Welch, R. A. (2006) Regulation of Type 1 Fimbriae by Unlinked FimB- and FimE-Like Recombinases in Uropathogenic Escherichia coli Strain CFT073. *Infect. Immun. 74*, 1072−1083.
(48) Blattner, F. R., Plunkett, G., Bloch, C. A., Perna, N. T., Burland, V., Riley, M., Collado-Vides, J., Glasner, J. D., Rode, C. K., Mayhew, G. F., Gregor, J., Davis, N. W., Kirkpatrick, H. A., Goeden, M. A., Rose, D. J., Mau, B., and Shao, Y. (1997) The Complete Genome Sequence of Escherichia coli K-12. *Science 277*, 1453−1462.
(49) Endy, D. (2005) Foundations for engineering biology. *Nature 438*, 449−453.
(50) Clancy, K., and Voigt, C. A. (2010) Programming cells: towards an automated "Genetic Compiler. *Curr. Opin. Biotechnol. 21*, 572−581.
(51) Burns, L. S., Smith, S. G. J., and Dorman, C. J. (2000) Interaction of the FimB Integrase with the fimS Invertible DNA Element in Escherichia coli In Vivo and In Vitro. *J. Bacteriol. 182*, 2953−2959.
(52) Wang, K. H., Sauer, R. T., and Baker, T. A. (2007) ClpS modulates but is not essential for bacterial N-end rule degradation. *Genes Dev. 21*, 403−408.
(53) Lou, C., Stanton, B., Chen, Y.-J., Munsky, B., and Voigt, C. A. (2012) Ribozyme-based insulator parts buffer synthetic circuits from genetic context. *Nat. Biotechnol. 30*, 1137−1142.
(54) Anderson, J. C., Voigt, C. A., and Arkin, A. P. (2007) Environmental signal integration by a modular AND gate. *Mol. Syst. Biol. 3*, 133.
(55) Saïda, F., Uzan, M., Odaert, B., and Bontems, F. (2006) Expression of highly toxic genes in E. coli: special strategies and genetic tools. *Curr. Protein Pept. Sci. 7*, 47−56.
(56) Zerbib, D., Gamas, P., Chandler, M., Prentki, P., Bass, S., and Galas, D. (1985) Specificity of insertion of IS1. *J. Mol. Biol. 185*, 517−524.
(57) Stanton, B. C., Nielsen, A. A. K., Tamsir, A., Clancy, K., Peterson, T., and Voigt, C. A. (2014) Genomic mining of prokaryotic repressors for orthogonal logic gates. *Nat. Chem. Biol. 10*, 99−105.


DOI: 10.1021/acssynbio.5b00170
*ACS Synth. Biol.* 2015, 4, 1361−1372

(58) Tamsir, A., Tabor, J. J., and Voigt, C. A. (2011) Robust multicellular computing using genetically encoded NOR gates and chemical "wires. *Nature 469*, 212−215.
(59) Anderson, J. C. (2009) Registry of Standard Biological Parts, www.partsregistry.org.
(60) Buchler, N. E., and Cross, F. R. (2009) Protein sequestration generates a flexible ultrasensitive response in a genetic network. *Mol. Syst. Biol. 5*, 272.
(61) Lee, T. H., and Maheshri, N. (2012) A regulatory role for repeated decoy transcription factor binding sites in target gene expression. *Mol. Syst. Biol. 8*, 576.
(62) Rhodius, V. A., Segall-Shapiro, T. H., Sharon, B. D., Ghodasara, A., Orlova, E., Tabakh, H., Burkhardt, D. H., Clancy, K., Peterson, T. C., Gross, C. A., and Voigt, C. A. (2013) Design of orthogonal genetic switches based on a crosstalk map of σs, anti-σs, and promoters. *Mol. Syst. Biol. 9*, 702.
(63) Sleight, S. C., Bartley, B. A., Lieviant, J. A., and Sauro, H. M. (2010) Designing and engineering evolutionary robust genetic circuits. *J. Biol. Eng. 4*, 12.
(64) Chen, Y.-J., Liu, P., Nielsen, A. A. K., Brophy, J. A. N., Clancy, K., Peterson, T., and Voigt, C. A. (2013) Characterization of 582 natural and synthetic terminators and quantification of their design constraints. *Nat. Methods 10*, 659−664.
(65) Canton, B., Labno, A., and Endy, D. (2008) Refinement and standardization of synthetic biological parts and devices. *Nat. Biotechnol. 26*, 787−793.
(66) Chalmers, R., Sewitz, S., Lipkow, K., and Crellin, P. (2000) Complete nucleotide sequence of Tn10. *J. Bacteriol. 182*, 2970−2972.
(67) Liu, J. D., and Parkinson, J. S. (1989) Genetics and sequence analysis of the pcnB locus, an Escherichia coli gene involved in plasmid copy number control. *J. Bacteriol. 171*, 1254−1261.
(68) Lopilato, J., Bortner, S., and Beckwith, J. (1986) Mutations in a new chromosomal gene of Escherichia coli K-12, pcnB, reduce plasmid copy number of pBR322 and its derivatives. *Mol. Gen. Genet. MGG 205*, 285−290.
(69) Masters, M., Colloms, M. D., Oliver, I. R., He, L., Macnaughton, E. J., and Charters, Y. (1993) The pcnB gene of Escherichia coli, which is required for ColE1 copy number maintenance, is dispensable. *J. Bacteriol. 175*, 4405−4413.
(70) Foster, T. J., Davis, M. A., Roberts, D. E., Takeshita, K., and Kleckner, N. (1981) Genetic organization of transposon Tn10. *Cell 23*, 201−213.
(71) Shearwin, K. E., Callen, B. P., and Egan, J. B. (2005) Transcriptional interference − a crash course. *Trends Genet. 21*, 339−345.
(72) Ghosal, D., Sommer, H., and Saedler, H. (1979) Nucleotide sequence of the transposable DNA-element IS2. *Nucleic Acids Res. 6*, 1111−1122.
(73) Golby, P., Davies, S., Kelly, D. J., Guest, J. R., and Andrews, S. C. (1999) Identification and characterization of a two-component sensor-kinase and response-regulator system (DcuS-DcuR) controlling gene expression in response to C4-dicarboxylates in Escherichia coli. *J. Bacteriol. 181*, 1238−1248.
(74) Barrick, J. E., Yu, D. S., Yoon, S. H., Jeong, H., Oh, T. K., Schneider, D., Lenski, R. E., and Kim, J. F. (2009) Genome evolution and adaptation in a long-term experiment with Escherichia coli. *Nature 461*, 1243−1247.
(75) Khan, A. I., Dinh, D. M., Schneider, D., Lenski, R. E., and Cooper, T. F. (2011) Negative Epistasis Between Beneficial Mutations in an Evolving Bacterial Population. *Science 332*, 1193−1196.
(76) Eichenbaum, Z., and Livneh, Z. (1998) UV light induces IS10 transposition in Escherichia coli. *Genetics 149*, 1173−1181.
(77) Twiss, E., Coros, A. M., Tavakoli, N. P., and Derbyshire, K. M. (2005) Transposition is modulated by a diverse set of host factors in Escherichia coli and is stimulated by nutritional stress. *Mol. Microbiol. 57*, 1593−1607.
(78) Sleight, S. C., Orlic, C., Schneider, D., and Lenski, R. E. (2008) Genetic Basis of Evolutionary Adaptation by Escherichia coli to Stressful Cycles of Freezing, Thawing and Growth. *Genetics 180*, 431−443.
(79) Gonçalves, G. A. L., Oliveira, P. H., Gomes, A. G., Prather, K. L. J., Lewis, L. A., Prazeres, D. M. F., and Monteiro, G. A. (2014) Evidence that the insertion events of IS2 transposition are biased towards abrupt compositional shifts in target DNA and modulated by a diverse set of culture parameters. *Appl. Microbiol. Biotechnol. 98*, 6609−6619.
(80) Gardner, T. S., Cantor, C. R., and Collins, J. J. (2000) Construction of a genetic toggle switch in Escherichia coli. *Nature 403*, 339−342.
(81) Kotula, J. W., Kerns, S. J., Shaket, L. A., Siraj, L., Collins, J. J., Way, J. C., and Silver, P. A. (2014) Programmable bacteria detect and record an environmental signal in the mammalian gut. *Proc. Natl. Acad. Sci. U. S. A. 111*, 4838−4843.
(82) Green, A. A., Silver, P. A., Collins, J. J., and Yin, P. (2014) Toehold Switches: De-Novo-Designed Regulators of Gene Expression. *Cell 159*, 925−939.
(83) Larson, M. H., Gilbert, L. A., Wang, X., Lim, W. A., Weissman, J. S., and Qi, L. S. (2013) CRISPR interference (CRISPRi) for sequence-specific control of gene expression. *Nat. Protoc. 8*, 2180−2196.
(84) Bikard, D., Jiang, W., Samai, P., Hochschild, A., Zhang, F., and Marraffini, L. A. (2013) Programmable repression and activation of bacterial gene expression using an engineered CRISPR-Cas system. *Nucleic Acids Res. 41*, 7429−7437.
(85) Tabor, J. J., Salis, H., Simpson, Z. B., Chevalier, A. A., Levskaya, A., Marcotte, E. M., Voigt, C. A., and Ellington, A. D. (2009) A Synthetic Genetic Edge Detection Program. *Cell 137*, 1272−1281.
(86) Caliando, B. J., and Voigt, C. A. (2015) Targeted DNA degradation using a CRISPR device stably carried in the host genome. *Nat. Commun. 6*, 6989.
(87) Lajoie, M. J., Rovner, A. J., Goodman, D. B., Aerni, H.-R., Haimovich, A. D., Kuznetsov, G., Mercer, J. A., Wang, H. H., Carr, P. A., Mosberg, J. A., Rohland, N., Schultz, P. G., Jacobson, J. M., Rinehart, J., Church, G. M., and Isaacs, F. J. (2013) Genomically Recoded Organisms Expand Biological Functions. *Science 342*, 357−360.
(88) Isaacs, F. J., Carr, P. A., Wang, H. H., Lajoie, M. J., Sterling, B., Kraal, L., Tolonen, A. C., Gianoulis, T. A., Goodman, D. B., Reppas, N. B., Emig, C. J., Bang, D., Hwang, S. J., Jewett, M. C., Jacobson, J. M., and Church, G. M. (2011) Precise Manipulation of Chromosomes in Vivo Enables Genome-Wide Codon Replacement. *Science 333*, 348−353.
(89) Elowitz, M. B., and Leibler, S. (2000) A synthetic oscillatory network of transcriptional regulators. *Nature 403*, 335−338.
(90) Cambray, G., Guimaraes, J. C., Mutalik, V. K., Lam, C., Mai, Q.-A., Thimmaiah, T., Carothers, J. M., Arkin, A. P., and Endy, D. (2013) Measurement and modeling of intrinsic transcription terminators. *Nucleic Acids Res. 41*, 5139−5148.
(91) Mutalik, V. K., Guimaraes, J. C., Cambray, G., Lam, C., Christoffersen, M. J., Mai, Q.-A., Tran, A. B., Paull, M., Keasling, J. D., Arkin, A. P., and Endy, D. (2013) Precise and reliable gene expression via standard transcription and translation initiation elements. *Nat. Methods 10*, 354−360.
(92) Stoebel, D. M., Hokamp, K., Last, M. S., and Dorman, C. J. (2009) Compensatory evolution of gene regulation in response to stress by Escherichia coli lacking RpoS. *PLoS Genet. 5*, e1000671.
(93) Glick, B. R. (1995) Metabolic load and heterologous gene expression. *Biotechnol. Adv. 13*, 247−261.
(94) Scott, M., Gunderson, C. W., Mateescu, E. M., Zhang, Z., and Hwa, T. (2010) Interdependence of Cell Growth and Gene Expression: Origins and Consequences. *Science 330*, 1099−1102.
(95) Sleight, S. C., and Sauro, H. M. (2013) Visualization of Evolutionary Stability Dynamics and Competitive Fitness of Escherichia coli Engineered with Randomized Multigene Circuits. *ACS Synth. Biol. 2*, 519−528.
(96) Bienick, M. S., Young, K. W., Klesmith, J. R., Detwiler, E. E., Tomek, K. J., and Whitehead, T. A. (2014) The Interrelationship


DOI: 10.1021/acssynbio.5b00170
*ACS Synth. Biol.* 2015, 4, 1361−1372

between Promoter Strength, Gene Expression, and Growth Rate. *PLoS One 9*, e109105.
(97) Gregg, C. J., Lajoie, M. J., Napolitano, M. G., Mosberg, J. A., Goodman, D. B., Aach, J., Isaacs, F. J., and Church, G. M. (2014) Rational optimization of tolC as a powerful dual selectable marker for genome engineering. *Nucleic Acids Res. 42*, 4779−4790.
(98) Csörgő, B., Fehér, T., Tímár, E., Blattner, F. R., and Pósfai, G. (2012) Low-mutation-rate, reduced-genome Escherichia coli: an improved host for faithful maintenance of engineered genetic constructs. *Microb. Cell Fact. 11*, 11.
(99) Umenhoffer, K., Fehér, T., Balikó, G., Ayaydin, F., Pósfai, J., Blattner, F. R., and Pósfai, G. (2010) Reduced evolvability of Escherichia coli MDS42, an IS-less cellular chassis for molecular and synthetic biology applications. *Microb. Cell Fact. 9*, 38.
(100) Darmon, E., and Leach, D. R. F. (2014) Bacterial Genome Instability. *Microbiol. Mol. Biol. Rev. 78*, 1−39.
(101) Foster, P. L. (2007) Stress-Induced Mutagenesis in Bacteria. *Crit. Rev. Biochem. Mol. Biol. 42*, 373−397.
(102) Wang, H. H., Isaacs, F. J., Carr, P. A., Sun, Z. Z., Xu, G., Forest, C. R., and Church, G. M. (2009) Programming cells by multiplex genome engineering and accelerated evolution. *Nature 460*, 894−898.
(103) Cong, L., Ran, F. A., Cox, D., Lin, S., Barretto, R., Habib, N., Hsu, P. D., Wu, X., Jiang, W., Marraffini, L. A., and Zhang, F. (2013) Multiplex Genome Engineering Using CRISPR/Cas Systems. *Science 339*, 819−823.
(104) Pijkeren, J. P. v., and Britton, R. A. (2014) Precision genome engineering in lactic acid bacteria. *Microb. Cell Fact. 13*, S10.
(105) Dalia, A. B., McDonough, E., and Camilli, A. (2014) Multiplex genome editing by natural transformation. *Proc. Natl. Acad. Sci. U. S. A. 111*, 8937−8942.
(106) Du, D., Wang, L., Tian, Y., Liu, H., Tan, H., and Niu, G. (2015) Genome engineering and direct cloning of antibiotic gene clusters via phage $\phi$BT1 integrase-mediated site-specific recombination in Streptomyces. *Sci. Rep. 5*, 8740.
(107) Galdzicki, M., Clancy, K. P., Oberortner, E., Pocock, M., Quinn, J. Y., Rodriguez, C. A., Roehner, N., Wilson, M. L., Adam, L., Anderson, J. C., Bartley, B. A., Beal, J., Chandran, D., Chen, J., Densmore, D., Endy, D., Grünberg, R., Hallinan, J., Hillson, N. J., Johnson, J. D., Kuchinsky, A., Lux, M., Misirli, G., Peccoud, J., Plahar, H. A., Sirin, E., Stan, G.-B., Villalobos, A., Wipat, A., Gennari, J. H., Myers, C. J., and Sauro, H. M. (2014) The Synthetic Biology Open Language (SBOL) provides a community standard for communicating designs in synthetic biology. *Nat. Biotechnol. 32*, 545−550.
(108) Jasiecki, J., and Węgrzyn, G. (2006) Transcription start sites in the promoter region of the Escherichia coli pcnB (plasmid copy number) gene coding for poly(A) polymerase I. *Plasmid 55*, 169−172.
(109) Lee, C., Kim, J., Shin, S. G., and Hwang, S. (2006) Absolute and relative QPCR quantification of plasmid copy number in Escherichia coli. *J. Biotechnol. 123*, 273−280.
(110) So, L., Ghosh, A., Zong, C., Sepúlveda, L. A., Segev, R., and Golding, I. (2011) General properties of transcriptional time series in Escherichia coli. *Nat. Genet. 43*, 554−560.
(111) Bernstein, J. A., Khodursky, A. B., Lin, P.-H., Lin-Chao, S., and Cohen, S. N. (2002) Global analysis of mRNA decay and abundance in Escherichia coli at single-gene resolution using two-color fluorescent DNA microarrays. *Proc. Natl. Acad. Sci. U. S. A. 99*, 9697−9702.


DOI: 10.1021/acssynbio.5b00170
*ACS Synth. Biol.* 2015, 4, 1361−1372